



Inhibition of HeLa cell growth by doxorubicin-loaded and tuftsin-conjugated arginate-PEG microparticles



Tianmu Hu^a, Anwar Saeed Ahmed Qahtan^a, Lei Lei, MD, PhD^{b, **}, Zhixin Lei^c,
Dapeng Zhao^a, Hemin Nie, PhD Professor^{a, d, *}

^a Institute of Bionanotechnology and Tissue Engineering, College of Life Sciences, Hunan University, Changsha, 410082, China

^b Department of Orthodontics, Xiangya Stomatological Hospital, Central South University, Changsha, 410008, China

^c Changsha DMY Medical Technology Co., Ltd, Changsha, 410005, China

^d Shenzhen Research Institute of Hunan University, Nanshan Hi-new Technology and Industry Park, Shenzhen, 518057, China

ARTICLE INFO

Article history:

Received 17 March 2017

Accepted 26 April 2017

Available online 6 May 2017

Keywords:

Controlled release

Tuftsin

Cellular uptake

Chemotherapy

ABSTRACT

In order to improve the release pattern of chemotherapy drug and reduce the possibility of drug resistance, poly(ethylene glycol amine) (PEG)-modified alginate microparticles (ALG-PEG MPs) were developed then two different mechanisms were employed to load doxorubicin (Dox): 1) forming Dox/ALG-PEG complex by electrostatic attractions between unsaturated functional groups in Dox and ALG-PEG; 2) forming Dox-ALG-PEG complex through EDC-reaction between the amino and carboxyl groups in Dox and ALG, respectively. Additionally, tuftsin (TFT), a natural immunomodulation peptide, was conjugated to MPs in order to enhance the efficiency of cellular uptake. It was found that the Dox-ALG-PEG-TFT MPs exhibited a significantly slower release of Dox than Dox/ALG-PEG-TFT MPs in neutral medium, suggesting the role of covalent bonding in prolonging Dox retention. Besides, the release of Dox from these MPs was pH-sensitive, and the release rate was observably increased at pH 6.5 compared to the case at pH 7.4. Compared with Dox/ALG-PEG MPs and Dox-ALG-PEG MPs, their counterparts further conjugated with TFT more efficiently inhibited the growth of HeLa cells over a period of 48 h, implying the effectiveness of TFT in enhancing cellular uptake of MPs. Over a period of 48 h, Dox-ALG-PEG-TFT MPs inhibited the growth of HeLa cells less efficiently than Dox/ALG-PEG-TFT MPs but the difference was not significant ($p > 0.05$). In consideration of the prolonged and sustained release of Dox, Dox-ALG-PEG-TFT MPs possess the advantages for long-term treatment.

© 2017 The Authors. Production and hosting by Elsevier B.V. on behalf of KeAi Communications Co., Ltd. This is an open access article under the CC BY-NC-ND license (<http://creativecommons.org/licenses/by-nc-nd/4.0/>).

1. Introduction

Chemotherapy drugs possess the ability to inhibit the growth of tumor cells. However, the efficacy of conventional chemotherapy was limited due to inefficient cellular uptake of drug and drug resistance induced by large drug dosages [1]. The latter challenges can be partially overcome through optimization of drug delivery vehicles. Biomedical scientists have made numerous efforts to

enable efficient drug trafficking through modifying the chemical and physical properties of drugs and their polymeric carriers, or adding biological features of tumor cells such as surface receptors onto delivery vehicles. Alginate (ALG) has been widely used in biomedical fields owing to its outstanding biosafety and biodegradability [1,2]. Furthermore, it is naturally anionic because of the presence of a large amount of carboxyl groups [3–6]. The anionic property enables the electrostatic interactions with cationic chemotherapy drugs and formation of ALG/drug complexes. In order to further prevent burst release of drug, polymers were employed to modify ALG [4,5,7]. In recent research, ALG has been modified with different types of polyethylene glycol (PEG) to improve its bioactivity and biocompatibility in emulsification [2,5,8,9], self-assembled polymeric micelles [10], microcapsule [11], hybrid microspheres, and cell microencapsulation [8,12,13]. PEG-modified ALG in these formulations exhibited improved

* Corresponding author. Institute of Bionanotechnology and Tissue Engineering, College of Life Sciences, Hunan University, Yuelu Mountain, Changsha, 410082, China.

** Corresponding author. Department of Orthodontics, Xiangya Stomatological Hospital, Central South University, 87 Xiangya Road, Changsha, 410008, China.

E-mail addresses: leilei8413@163.com (L. Lei), niehemin@hnu.edu.cn (H. Nie).

Peer review under responsibility of KeAi Communications Co., Ltd.

pharmacokinetic properties of Dox through providing physical encapsulation. Actually, PEG-modified ALG (ALG-PEG) can be further improved by adding functional units with pH-sensitivity, photosensitivity or other responsive linkages and thus achieve improved release pattern of chemotherapy drugs [1,2,14,15].

Tuftsins (TFT), a Thr-Lys-Pro-Arg tetrapeptide, is a natural immunomodulation peptide formed by enzymatic cleavage of the Fc portion of immunoglobulin (IgG). TFT has been shown to interact with neuropilin-1 (NRP-1) receptors on macrophages, and around 72,000 binding sites are available on the surface of macrophages for this peptide [16]. As NRP-1 expression level has been shown elevated in a number of human patient tumor samples, including brain, prostate, breast, colon, and lung cancers [17–19], exogenous TFT would tend to be at a higher chance of binding tumor cells than normal cells. As such, TFT is of promise in delivering chemotherapy drugs in terms of targeting NRP-1 on tumor cell surface and mediating cellular uptake.

This study focused on the roles of Dox loading mechanisms (covalent binding and electrostatic attraction) and TFT conjugation in ALG-PEG microparticle-mediated chemotherapy. Particularly, PEG-ALG microparticles (ALG-PEG MPs) were modified in two ways: 1) with different types of linkages: electrostatic attractions between Dox and ALG-PEG (forming Dox/ALG-PEG), and chemical reaction between amino groups in Dox and carboxyl in ALG by EDC-chemistry (forming Dox-ALG-PEG); 2) with or without TFT conjugation (Dox/ALG-PEG, Dox/ALG-PEG-TFT, Dox-ALG-PEG and Dox-ALG-PEG-TFT). The release rates of Dox from different types of complexes in neutral and acidic medium were characterized. Furthermore, relative inhibition efficiencies of different MPs in HeLa cell growth over a period of 48 h were investigated.

2. Materials and methods

2.1. Materials

Sodium ALG was purchased from Sangon Biotech (Shanghai, China). Poly(ethylene glycol amine) (PEG, 4 arms, $M_w = 10$ kDa) was supplied by Sinopeg Biotech (Xiamen, China). Tuftsins, and 3-(4,5-dimethylthiazol-2-yl)-2,5-diphenyl tetrazolium bromide (MTT) were obtained from Sigma Aldrich. Doxorubicin hydrochloride (Dox) was purchased from Sangon Biotech (Shanghai, China). Triethylamine (TEA), N-dimethylformamide (DMF), and dimethyl sulfoxide (DMSO) were obtained from J&K Scientific (Beijing, China). N-ethyl-N' (3-dimethylaminopropyl) carbodiimide hydrochloric acid (EDC), N-hydroxysuccinimide (NHS) and phosphate buffered saline (PBS) were purchased from Aladdin Bio-Chem Technology (Shanghai, China). Penicillin, streptomycin and Trypsin EDTA were purchased from Gibco. All the chemicals were of analytical grade. Deionized water was used throughout the experiments. Human cervical cancer (HeLa) cells were maintained in Dulbecco's modified Eagle's medium (DMEM) supplied by Gibco, supplemented with 10% fetal bovine serum (FBS) and antibiotics (Penicillin-Streptomycin solution) under standard cell culture conditions (humidified, 37 °C, 5% CO₂).

2.2. Preparation of ALG-PEG and Dox-ALG-PEG

ALG-PEG was synthesized via EDC reaction [20]. Briefly, 0.25 mg of ALG was dissolved into 25 mL DMSO and mixed with 15 mL distilled water in a 100-mL conical flask, followed by magnetic stirring for 12 h at room temperature [14]. Then, EDC·HCl and NHS were added into the emulsion at molar ratio of 1/1.2/1.2 (ALG/EDC·HCl/NHS) under continuous stirring [15]. The solution was divided into two equal parts and PEG was added into both solutions at a final concentration of 2 mg/mL under continuous stirring. In

the first solution, the solution was stirred overnight at room temperature and precipitated by centrifugation under 19,750 g for 5 min to remove the leftover PEG and ALG [1]. Then, the solution was loaded into a dialysis bag (MWCO 8000–14000 Da) and dialyzed against distilled water for 2 days to remove residual reagents before obtaining ALG-PEG [10,14]. The second solution was incubated for 2 min under magnetic stirring, followed by adding Dox to a final concentration of 1 mg/mL, and then stirred overnight at room temperature. The mixture was precipitated by centrifugation under 19,750 g for 5 min to remove free Dox. Then, the solution was placed into a dialysis bag (MWCO 8000–14000 Da) and dialyzed against distilled water for 2 days to remove the leftover substances before Dox-ALG-PEG conjugates were obtained. ALG-PEG and Dox-ALG-PEG microparticles (MPs) were lyophilized before characterizations analysis (Scheme 1).

2.3. Preparation of ALG-PEG-TFT and Dox-ALG-PEG-TFT

0.4 mg of lyophilized ALG-PEG and Dox-ALG-PEG MPs, respectively were added into 20 mL of TFT solution (1 mg/mL). The carboxyl groups in TFT were activated beforehand via EDC reaction overnight under magnetic stirring at room temperature. The mixture was stirred for 12 h at room temperature, then transferred into a dialysis bag (MWCO 8000–14000 Da) and dialyzed against distilled water for 2 days to remove free TFT and other reagents before Dox-ALG-PEG-TFT and ALG-PEG-TFT were obtained by lyophilization (Scheme 1).

2.4. Preparation of Dox/ALG-PEG-TFT and Dox-ALG-PEG MPs

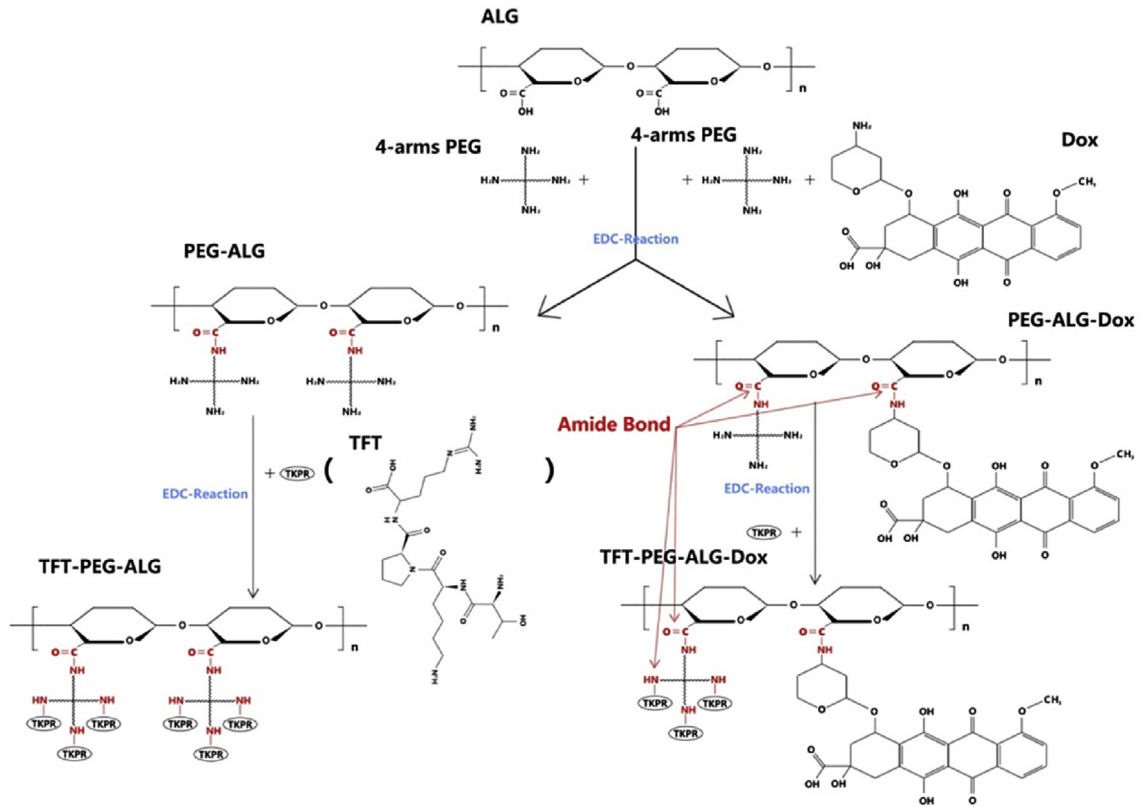
Dox·HCl (1 mg/mL) was dissolved in DMF·TEA (DMF/TEA molar ratio = 2/3) under stirring to remove HCl [1,14,15]. The solution was then added to ALG-PEG-TFT and ALG-PEG solution respectively and stirred overnight. Subsequently, the suspension (in red color) was precipitated by centrifugation under 19,750 g for 5 min to remove free Dox, and then transferred into a dialysis bag (Mw. 8000–14000 kDa) and dialyzed against distilled water for 2 days to remove leftover reagents. The medium was changed frequently, and the dialyzed solution was lyophilized to obtain Dox/ALG-PEG-TFT and Dox-ALG-PEG MPs, respectively (Scheme 2).

2.5. Characterization of the MPs

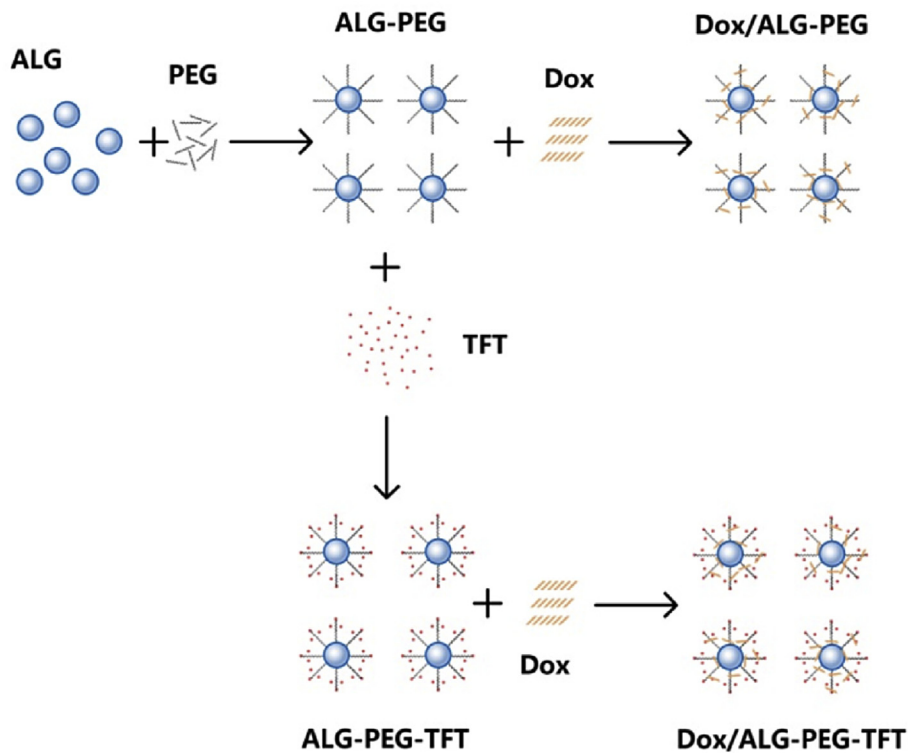
The structures of ALG-PEG, Dox/ALG-PEG, Dox-ALG-PEG, ALG-PEG-TFT, Dox/ALG-PEG-TFT, and Dox-ALG-PEG-TFT were characterized using a UV-vis spectrophotometer (UV-4802H, Unic, US) and a FT-IR spectrometer (Bio-Rad FTS-6000, US). The size and surface charge (zeta potential) of the samples were measured at room temperature using Zetasizer Nano ZS90 (Malvern Instruments, UK). Before measurement, the samples were suspended in distilled water and subjected to ultrasound sonication (Branson 2510, 100 w) for 10 min. In order to obtain the loading capacity of Dox on Dox/ALG-PEG, Dox-ALG-PEG, Dox/ALG-PEG-TFT and Dox-ALG-PEG-TFT, absorbance of the samples at 480 nm were measured by Micro spectrophotometer (NSPL3488A/NSPL3276, Zeiss, US) and the absorbance of respective carrier (ALG-PEG or ALG-PEG-TFT) was subtracted, then the corresponding Dox concentration was calculated based on a standard curve of pure Dox at 480 nm.

2.6. Drug release

In vitro release of Dox from different MPs was monitored by a dialysis method [21]. Briefly, a specific amount of MPs were loaded into a Spectro/Por dialysis membrane bag (MWCO: 2000 Da) and



Scheme 1. Route for synthesis of ALG-PEG, ALG-PEG-TFT, Dox-ALG-PEG and Dox-ALG-PEG-TFT via EDC reaction.



Scheme 2. Route for synthesis of Dox/ALG-PEG and Dox/ALG-PEG-TFT.

stored into a centrifuge tube with 50 ml of PBS at different pH values (pH = 7.4 as the neutral physiological medium; pH = 6.5 as

the acidic medium that simulated the physiological conditions in tumor microenvironments). The whole system was then placed in

an orbital shaker bath (ZWYR-D2403, Shanghai Zhicheng Analytical Instrument, China) maintained at 37 °C and 120 rpm. At specific time intervals (6, 12, 24, 48, 72, 96, 120, 144, 168, 192, 216, and 240 h), 5.0 ml of the incubation medium was withdrawn for analysis and supplemented with 5.0 ml of fresh PBS medium. The concentrations of Dox at specific intervals were quantified using high performance liquid chromatography (HPLC, LC-20AT, Shimadzu, Japan), and the release of Dox at specific intervals in response to different pH values were recorded and compared.

2.7. Cell inhibition ability of MPs

The efficiency of different MPs in inhibiting the growth of HeLa cells was assessed by MTT method. Cells were seeded at approximately 4×10^3 cells/well on a 96-well plate, and incubated with Dox·HCl, Dox/ALG-PEG, Dox-ALG-PEG, Dox/ALG-PEG-TFT, or Dox-ALG-PEG-TFT MPs for 24 and 48 h respectively. Cells were washed with PBS and treated with 20 μ L of MTT solution (5 mg/mL in PBS) for an additional 4 h at 37 °C. Then the medium was removed and 100 μ L of DMSO was added to dissolve the MTT formazan crystals. The absorbance at 490 nm was measured to calculate the cellular viability with the untreated cells as control.

2.8. Statistical analysis

All the experiments were performed independently at least three times and representative experimental results were shown. Data were analyzed using SPSS Statistics 17.0 for one-way analysis of variance (ANOVA), followed by Tukey's HSD post hoc test. Differences were considered significant when $P < 0.05$.

3. Results

3.1. Characterization of MPs

Fig. 1 shows a new peak of ALG-PEG compared to ALG and PEG in UV-vis spectra, suggesting the formation of amide bonds between ALG and PEG via EDC reaction [5,15]. After further conjugation, Dox-ALG-PEG and ALG-PEG-TFT preserved the characteristic peak of Dox shown at 480 nm and 230 nm, and the characteristic peak of TFT at 197 nm, respectively, indicating that Dox and TFT were successfully conjugated onto ALG-PEG backbone. Furthermore, Dox-ALG-PEG-TFT and Dox/ALG-PEG-TFT both showed the characteristic peak of TFT at 197 nm, but Dox/ALG-PEG-TFT failed to show one of the characteristic peak for Dox at 480 nm. This absence may be attributed to the electrostatic attraction between Dox and ALG-PEG-TFT and resultant steric shielding on Dox.

The C-N stretching vibrations ranged between 1000 and 800 cm^{-1} confirmed the formation of ALG-PEG through amide bonds between -COOH of ALG and -NH₂ of PEG (Fig. 2). The peak at 1300 cm^{-1} standing for R₂NH- also suggested the formation of amide bonds between the -NH₂ of PEG and -COOH of TFT, and between the -NH₂ of Dox and -COOH of ALG. After being modified with TFT or Dox, the intensity of C-C stretchings became sharper and emerged at 1095 cm^{-1} and 1033 cm^{-1} , respectively. The characteristic peak attributed to C=O bonds in ALG-PEG-TFT was shifted from 1647 to 1781 cm^{-1} in Dox-ALG-PEG-TFT. Accordingly, the observations showed that ALG-PEG-TFT, Dox-ALG-PEG, and Dox-ALG-PEG-TFT were fabricated via EDC reaction based on ALG-PEG.

The diameters and polydispersity indexes (PDI) of different MPs were characterized in distilled water. As shown in Table 1, the mean hydrodynamic diameters of ALG-PEG MPs were 554.7 nm, while the diameters of the modified MPs were increased to 800.7 nm and 895.4 nm for Dox/ALG-PEG-TFT MPs and Dox-ALG-PEG-TFT MPs,

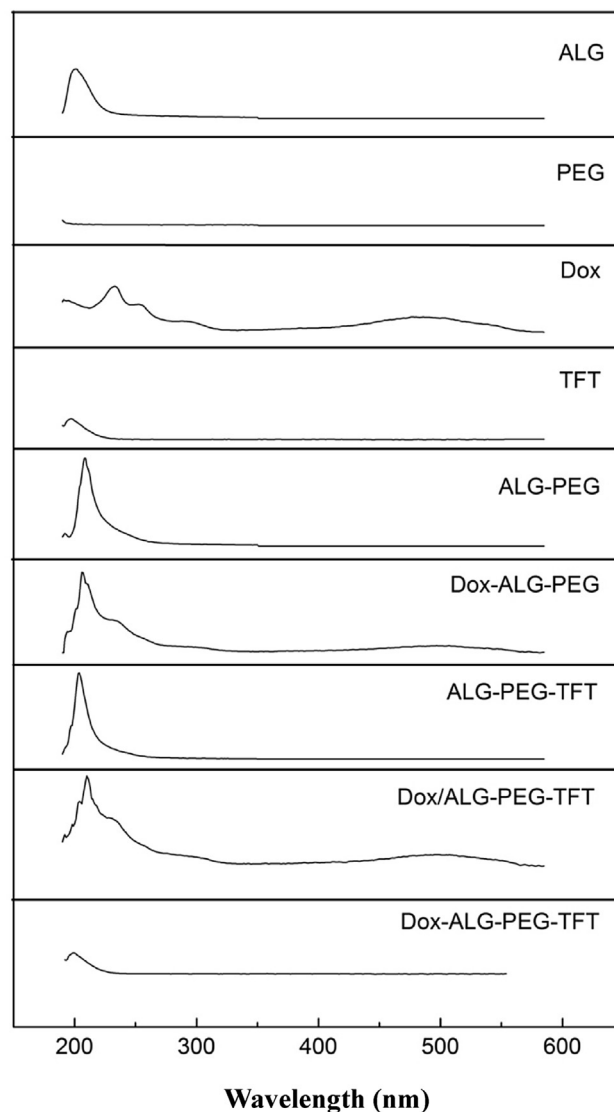


Fig. 1. UV-vis spectra of different MPs, including ALG-PEG, Dox-ALG-PEG, ALG-PEG-TFT, Dox-ALG-PEG-TFT, and Dox/ALG-PEG-TFT.

respectively. Based on the polydispersity index (PDI) of the MPs showed in Table 1, the MPs were monodisperse and uniform. Additionally, the loading capacity of Dox for different MPs was strongly affected by loading methods. As shown in Table 1, relatively more Dox was loaded in the MPs via electrostatic interactions than in the MPs via covalent linkage. Among all the MPs, Dox/ALG-PEG MPs encapsulated the highest amount of Dox. Zeta potential is a main factor when assessing the stability of a colloidal dispersion. According to Fig. 3, all of the synthesized MPs, including Dox/ALG-PEG and Dox/ALG-PEG-TFT carried negative charges, attributed to the carboxyl groups of ALG. Owing to the charge properties of ALG-PEG and ALG-PEG-TFT, Dox/ALG-PEG and Dox/ALG-PEG-TFT were formed via self-assembling with positively charged Dox. As negatively charged surfaces induce a low plasma protein bioadhesion and low rate of non-specific cellular uptake, these ALG-PEG-based MPs may possess advanced pharmaceutical properties.

3.2. In vitro drug release

Fig. 4 shows the *in vitro* release profiles of Dox/ALG-PEG-TFT and

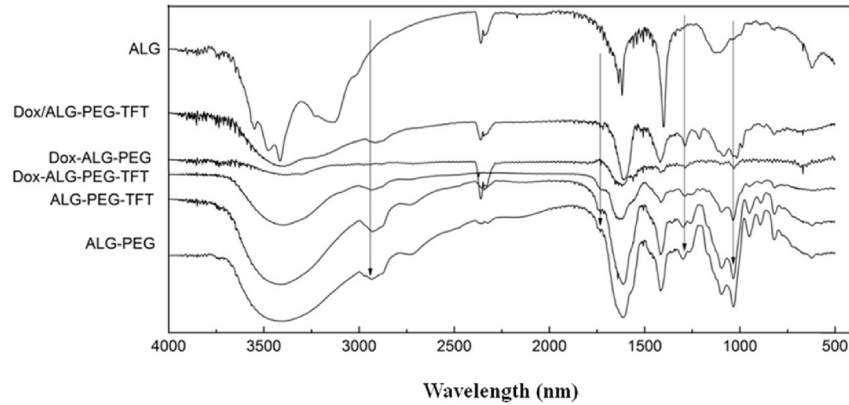


Fig. 2. FT-IR spectra of different MPs, including ALG-PEG, Dox-ALG-PEG, ALG-PEG-TFT, Dox-ALG-PEG-TFT, and Dox/ALG-PEG-TFT.

Table 1
Characterization of different microparticles.

Sample	Diameter (nm)	PDI	Loading capacity of Dox (%)
ALG	1395	0.469	—
ALG-PEG	554.7	0.199	—
ALG-PEG-TFT	644.1	0.008	—
DOX/ALG-PEG	894	0.379	17.1
DOX/ALG-PEG-TFT	800.7	0.239	10.2
DOX-ALG-PEG	807.7	0.426	9.3
DOX-ALG-PEG-TFT	895.4	0.334	4.8

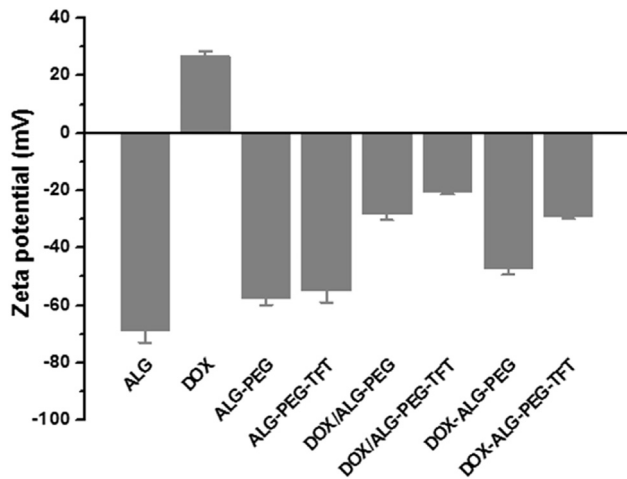


Fig. 3. Zeta potential of different MPs, including ALG-PEG, ALG-PEG-TFT, Dox/ALG-PEG, Dox/ALG-PEG-TFT, Dox-ALG-PEG, and Dox-ALG-PEG-TFT (n = 3).

Dox-ALG-PEG-TFT in simulated normal physiological environment (pH 7.4) and tumor microenvironment (pH 6.5). Dox/ALG-PEG-TFT and Dox-ALG-PEG-TFT released Dox at pH 7.4 but exhibited differentiated drug release profiles over time. Due to the low bonding energy between Dox and carrier, the release of Dox in the electrostatic attraction groups was faster than that in the covalent groups. After 240 h of release at pH 7.4, the on-the-spot concentrations of Dox reached 0.15 mg/mL and 0.089 mg/mL for Dox/ALG-PEG-TFT and Dox-ALG-PEG-TFT, respectively. On the contrast, after a same time period of release at pH 6.5, the on-the-spot concentrations of Dox climbed up to 0.23 mg/mL and 0.144 mg/mL for Dox/ALG-PEG-TFT and Dox-ALG-PEG-TFT, respectively. These comparisons suggested the critical role of linkage types between Dox and carriers in release patterns. Dox release from Dox/ALG-PEG-TFT was

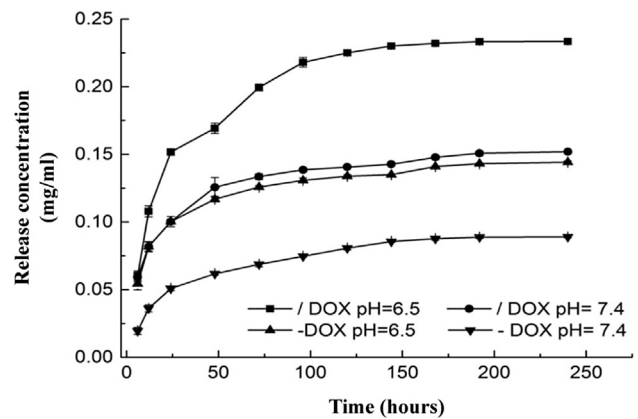


Fig. 4. *In vitro* release of Dox-ALG-PEG-TFT and Dox/ALG-PEG-TFT MPs under acidic (pH 6.5) and neutral (pH 7.4) conditions at 37 °C. Each point represents average value \pm S.D. (n = 3).

sensitive to pH decrease because the electrostatic interaction between Dox and carrier was transformed and weakened in acidic environment. Dox-ALG-PEG-TFT showed the sensitivity to pH decrease because the covalent amides between Dox and ALG-PEG-TFT in Dox-ALG-PEG-TFT was reversible and the hydrolysis of amide was enhanced in acidic environment compared with neutral environment [14,15]. For each kind of linkage, Dox was released faster in acidic environment than in neutral environment. As expected, the MPs may release more efficiently in tumor sites and therefore cause less damage to neighboring normal tissues. Besides, regardless of pH values, the stronger bonds in Dox-ALG-PEG-TFT MPs enabled the longer retaining of Dox and may help achieve longer-term biological effects compared with Dox/ALG-PEG-TFT MPs.

3.3. Cytotoxicity assessment of carrier materials and TFT

Fig. 5 shows that ALG-PEG possessed relatively lower cytotoxicity than ALG (80% vs. 69%, $p > 0.05$), suggesting that ALG-PEG is relatively safer as a drug delivery vehicle. It's worth mentioning that free TFT exhibited no significant toxicity to HeLa cells in a broad range of concentrations (0.0002 mg/ml - 0.02 mg/ml). As a result, no significant difference in cytotoxicity was detected between ALG-PEG and ALG-PEG-TFT ($p > 0.05$).

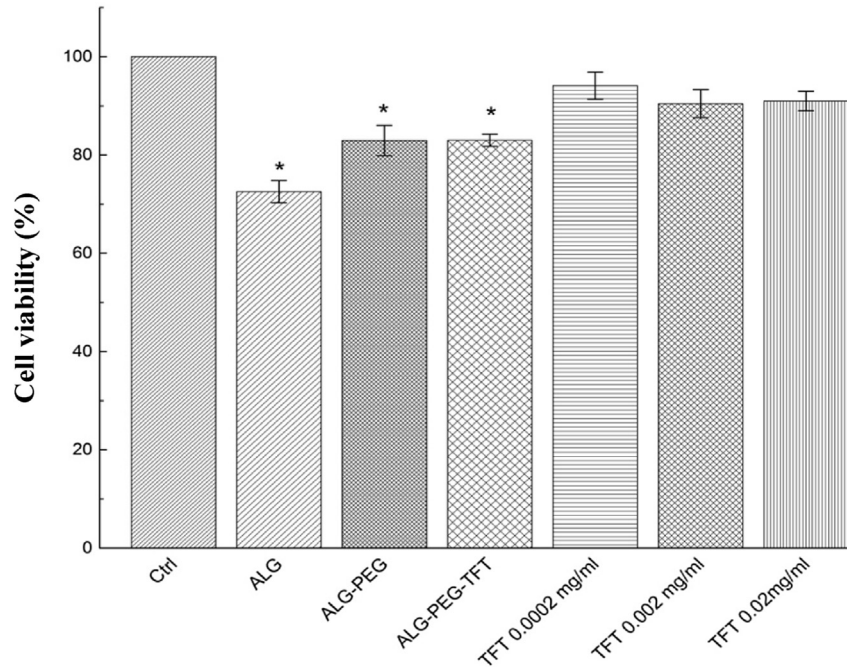


Fig. 5. Cytotoxicity of ALG, ALG-PEG, ALG-PEG-TFT, and different dosages of free TFT (0.0002–0.02 mg/ml). The asterisks stand for significant difference compared with control (* $p < 0.05$).

3.4. Inhibition of HeLa cell growth

The influence of different MPs on HeLa cell growth was analyzed via MTT assay. As shown in Fig. 6, the MPs loaded with Dox (Dox/ALG-PEG, Dox-ALG-PEG, Dox/ALG-PEG-TFT and Dox-ALG-PEG-TFT)

remarkably inhibited the growth of HeLa cells, but in different efficiencies. Cell viabilities in Dox-ALG-PEG and Dox/ALG-PEG groups were comparable at 24 h (Fig. 6a) and 48 h (Fig. 6b), but much higher than their counterpart groups conjugated with TFT (Dox-ALG-PEG-TFT and Dox/ALG-PEG-TFT, respectively). As discussed

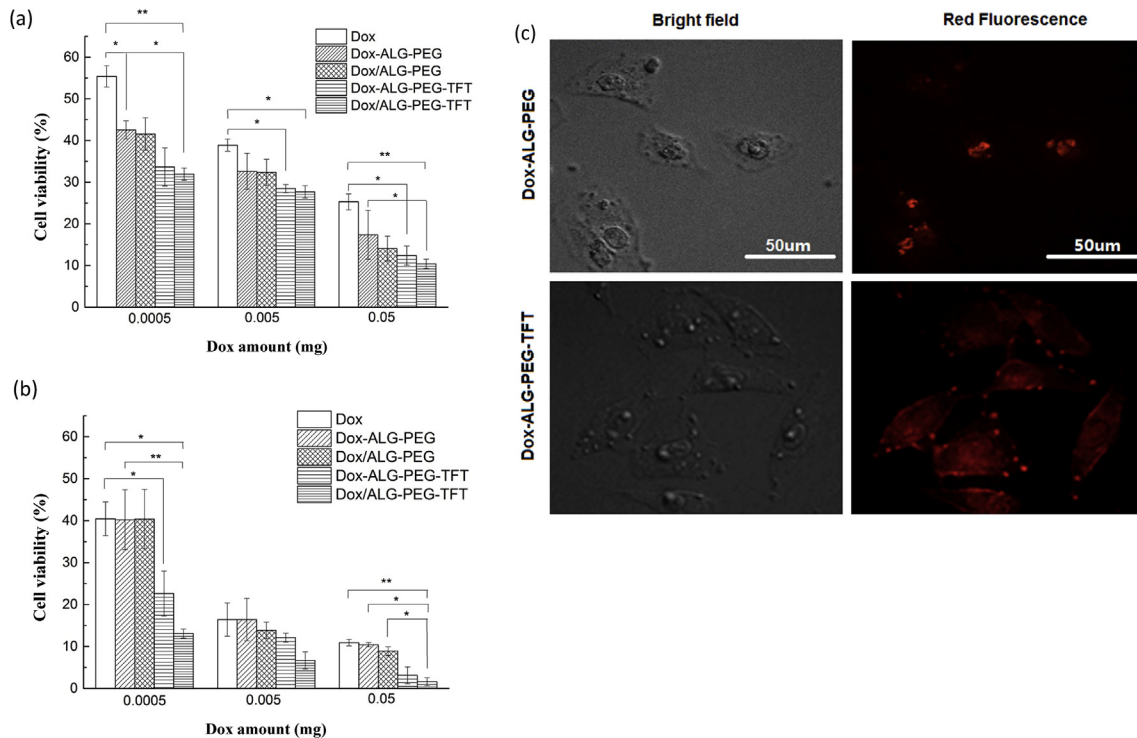


Fig. 6. Inhibition of HeLa cells over a period of 24 h (a) and 48 h (b) by different MPs, with non-treated cells as control. The asterisks stand for significant difference compared with free Dox group (* $p < 0.05$, ** $p < 0.01$). Comparison of cellular uptake efficiency between Dox-ALG-PEG and Dox-ALG-PEG-TFT at 6 h (c).

earlier, TFT itself showed no significant cytotoxicity towards HeLa cells. Therefore, further investigations were warranted on the mechanism for enhancement of TFT in the inhibition of HeLa cells. As shown in Fig. 6c, in a same period of time, Dox-ALG-PEG-TFT particles were relatively more efficiently uptaken by HeLa cells compared with Dox-ALG-PEG particles. Dox/ALG-PEG-TFT group showed the highest inhibition efficiency, and the effect stayed at a high level within 48 h in a broad range of concentration of Dox (0.0005–0.05 mg/mL). These results suggested that the release rate of electrostatic attraction group was superior in short term. The difference should be attributed to the lower bonding energy of electrostatic attraction between Dox and carrier, which holds drug looser than chemical bonds.

Dox-loaded ALG-PEG MPs, including Dox/ALG-PEG and Dox-ALG-PEG, remarkably inhibited the growth of HeLa cells *in vitro*, but absence of cell adhesion units may limit their utility *in vivo*. In previous studies, TFT was known as a tetrapeptide that could stimulate phagocytosis and enhance immune system and anti-tumor activity via binding to specific receptors on the surface of macrophages and polymorphonuclear leukocytes. Our study suggested that TFT itself exhibited no significant cytotoxicity to HeLa cells, but it possessed the ability to magnify the inhibition efficiency of Dox-loaded MPs. The enhancement provided a new horizon for the application of TFT and it should be attributed to related receptors on the surface of HeLa cells, which was up-regulated compared to normal cells. However, further investigations are warranted to uncover the mechanisms.

4. Conclusions

In the current work, four types of MPs based on ALG-PEG were successfully synthesized through electrostatic attraction or chemical reaction, and it was found that the Dox-ALG-PEG-TFT MPs exhibited a significantly slower release of Dox than Dox/ALG-PEG-TFT MPs in PBS, suggesting the role of covalent bonding in prolonging Dox retention. Besides, the release of Dox from these MPs was pH-sensitive, and the release rate was observably increased at pH 6.5 compared to the case at pH 7.4. Compared with Dox/ALG-PEG and Dox-ALG-PEG MPs, their counterparts further conjugated with TFT more efficiently inhibited the growth of HeLa cells over a period of 48 h, implying the effectiveness of TFT in enhancing Dox trafficking. Over a period of 48 h, Dox-ALG-PEG-TFT MPs inhibited the growth of HeLa cells less efficiently than Dox/ALG-PEG-TFT MPs but the difference was not significant ($p > 0.05$). In view of the prolonged and sustained release of Dox, Dox-ALG-PEG-TFT MPs possess the advantages for longer-term treatment.

Acknowledgments

This study was funded by the National Natural Scientific Foundation of China (31670997), Natural Science Foundation of Hunan Province (2015JJ1007), and Basic Research Program of Shenzhen City (JCYJ20160530193417959). The authors wish to confirm that there are no conflicts of interest associated with this publication.

References

- [1] M. Gonçalves, P. Figueira, D. Maciel, J. Rodrigues, X. Qu, C. Liu, H. Tomás, Y. Li, pH-sensitive Laponite[®]/doxorubicin/alginate nanohybrids with improved anticancer efficacy, *Acta Biomater.* 10 (1) (2014) 300–307.
- [2] L.A. Wells, H. Sheardown, Photosensitive controlled release with polyethylene glycol–anthracene modified alginate, *Eur. J. Pharm. Biopharm.* 79 (2) (2011) 304–313.
- [3] K.Y. Lee, D.J. Mooney, Alginate: properties and biomedical applications, *Prog. Polym. Sci.* 37 (1) (2012) 106–126.
- [4] S.N. Pawar, K.J. Edgar, Alginate derivatization: a review of chemistry, properties and applications, *Biomaterials* 33 (11) (2012) 3279–3305.
- [5] T.X. Miao, K.S. Rao, J.L. Spees, R.A. Oldinski, Osteogenic differentiation of human mesenchymal stem cells through alginate-graft-poly(ethylene glycol) microsphere-mediated intracellular growth factor delivery, *J. Control Release* 192 (2014) 57–66.
- [6] Cheong Hian Goh, Paul Wan Sia Heng, Lai Wah Chan, Alginates as a useful natural polymer for microencapsulation and therapeutic applications, *Carbohydr. Polym.* 88 (1) (2012) 1–12.
- [7] Ning Lin, Jin Huang, Peter R. Chang, Liangdong Feng, Jiahui Yu, Effect of polysaccharide nanocrystals on structure, properties, and drug release kinetics of alginate-based microspheres, *Colloids Surfaces B Biointerfaces* 85 (2) (2011) 270–279.
- [8] Redouan Mahou, Christine Wandrey, Alginate–Poly(ethylene glycol) hybrid microspheres with adjustable physical properties, *Macromolecules* 43 (3) (2010) 1371–1378.
- [9] M. Davidovich-Pinhas, H. Bianco-Peled, Physical and structural characteristics of acrylated poly(ethylene glycol)-alginate conjugates, *Acta Biomater.* 7 (7) (2011) 2817–2825.
- [10] D.G. Ahn, J. Lee, S.Y. Park, Y.J. Kwark, K.Y. Lee, Doxorubicin-loaded alginate-g-poly(N-isopropylacrylamide) micelles for cancer imaging and therapy, *ACS Appl. Mater. Interfaces* 6 (24) (2014) 22069–22077.
- [11] S.J. Chang, C.H. Lee, C.Y. Hsu, Y.J. Wang, Biocompatible microcapsules with enhanced mechanical strength, *J. Biomed. Mater. Res.* 59 (1) (2002) 118–126.
- [12] R. Mahou, N.M. Tran, M. Dufresne, C. Legallais, C. Wandrey, Encapsulation of Huh-7 cells within alginate-poly(ethylene glycol) hybrid microspheres, *J. Mater. Sci. Mater. Med.* 23 (1) (2012) 171–179.
- [13] K. Knop, R. Hoogenboom, D. Fischer, U.S. Schubert, Poly(ethylene glycol) in drug delivery: pros and cons as well as potential alternatives, *Angewandte Chemie Int. Ed. Engl.* 49 (36) (2010) 6288–6308.
- [14] Hua Guo, Quanyong Lai, Wei Wang, Yukun Wu, Chuangnian Zhang, Yuan Liu, Zhi Yuan, Functional alginate nanoparticles for efficient intracellular release of doxorubicin and hepatoma carcinoma cell targeting therapy, *Int. J. Pharm.* 451 (1–2) (2013) 1–11.
- [15] C.N. Zhang, W. Wang, T. Liu, Y.K. Wu, H. Guo, P. Wang, Q. Tian, Y.M. Wang, Z. Yuan, Doxorubicin-loaded glycyrrhetic acid-modified alginate nanoparticles for liver tumor chemotherapy, *Biomaterials* 33 (2012) 2187–2196.
- [16] Z. Bar-Shavit, Y. Stabinsky, M. Fridkin, R. Goldman, Tuftsin-macrophage interaction: specific binding and augmentation of phagocytosis, *J. Cell. Physiol.* 100 (1) (1979) 55–62.
- [17] Mitra Fakhari, Dieter Pullirsch, Dietmar Abraham, Kurosh Paya, Reinhold Hofbauer, Paul Holzfeind, Michael Hofmann, Seyedhossein Aharinejad, Selective upregulation of vascular endothelial growth factor receptors neuropilin-1 and -2 in human neuroblastoma, *Cancer* 94 (1) (2002) 258–263.
- [18] R.E. Bachelder, A. Crago, J. Chung, M.A. Wendt, L.M. Shaw, G. Robinson, A.M. Mercurio, Vascular endothelial growth factor is an autocrine survival factor for neuropilin-expressing breast carcinoma cells, *Cancer Res.* 61 (2001) 5736–5740.
- [19] T.M. Hong, Y.L. Chen, Y.Y. Wu, A. Yuan, Y.C. Chao, Y.C. Chung, M.H. Wu, S.C. Yang, S.H. Pan, J.Y. Shih, W.K. Chan, P.C. Yang, Targeting neuropilin 1 as an antitumor strategy in lung cancer, *Clin. Cancer Res. Off. J. Am. Assoc. Cancer Res.* 13 (16) (2007) 4759–4768.
- [20] N. Nakajima, Y. Ikada, Mechanism of amide formation by carbodiimide for bioconjugation in aqueous media, *Bioconjugate Chem.* 6 (1) (1995 Jan-Feb) 123–130.
- [21] H.M. Nie, Z.G. Dong, D.Y. Arifin, Y. Hu, C.H. Wang, Core/shell microspheres via coaxial electrohydrodynamic atomization for sequential and parallel release of drugs, *J. Biomed. Mater. Res. A* 95A (2010) 709–716.